NSRRC - J0532Ψ (2016)

Nanoscale

COMMUNICATION

View Article Online
View Journal | View Issue

Published on 30 September 2016. Downloaded by National Chiao Tung University on 27/10/2016 02:04:51.

CrossMark

Cite this: *Nanoscale*, 2016, **8**, 17427

Received 2nd August 2016,
Accepted 13th September 2016

DOI: 10.1039/c6nr06106k

www.rsc.org/nanoscale

Solution-processed ultra-low-*k* thin films comprising single-walled aluminosilicate nanotubes†

An-Chih Yang,[a] Yun-Shiuan Li,[b] Chon Hei Lam,[a] Heng-Yu Chi,[a] I-Chun Cheng*[b] and Dun-Yen Kang*[a]

Nanotube-based ultra-low-*k* thin films with high Young's modulus composed of single-walled aluminosilicate nanotubes (AlSiNTs) and a trace amount of poly(vinyl alcohol) (PVA) have been developed. The dehydrated AlSiNT film possesses a relative permittivity of 1.05, and a Young's modulus of 25 GPa, which exceed those of most existing ultra-low-*k* materials.

Low-dielectric-constant (low-*k*, $k < 4.0$) thin films play a key role in nanometer-scale manufacturing. They are valued for their ability to reduce signal delays, power consumption, and crosstalk noise between electrodes and adjacent devices.[1–3] They are also desirable as interlayer dielectrics in three dimensional integrated circuits. Sub-90 nm manufacturing can only be realized using ultra-low-*k* materials ($k < 2.0$) in the frequency range from 1 kHz–10 GHz.[4] Polymers[5–7] and nanoporous materials[8–11] with a wide bandgap are two types of materials used in the fabrication of low-*k* and ultra-low-*k* thin films. Polymeric materials are easily processed; however, they suffer from low thermal stability and poor mechanical properties.[3] Specifically, low-*k* thin films require a Young's modulus greater than 6 GPa for micro/nanoelectronics;[12,13] however, most existing polymeric thin films have a Young's modulus of only 1 GPa.[7] Low-*k* thin films made of nanoporous materials, such as zeolites,[14–17] metal–organic frameworks (MOFs),[18–21] and mesoporous silica,[22–25] have higher elastic modulus than polymeric thin films. The Young's modulus values of nanoporous low-*k* thin films are in the range of 5–20 GPa. Three-dimensional (3D) nanoporous materials composed of wide-bandgap materials (organic moieties in MOFs and metal oxides in zeolites) with nanopores filled with air, whose *k* value is close to 1. This results in thin films made of these materials with a low overall dielectric constant. The strategies used to lower the *k* value typically involve increasing the number or size of pores in the thin films; however, both of these measures tend to undermine mechanical integrity.[26,27] Another approach involves the use of one-dimensional (1D) nanoporous materials in the form of nanotubes, which provide high porosity and excellent mechanical properties. Previous studies have indicated that the Young's modulus of single-walled carbon nanotubes can exceed 1000 GPa,[28–31] and that of single-walled aluminosilicate nanotubes can exceed 300 GPa.[32–35]

Carbon nanotubes (CNTs) have been investigated since 1991.[36] These structures possess high porosity and excellent mechanical properties; however, their narrow bandgap (bandgap < 2 eV)[37] means that they are ill-suited to the low-*k* films found in electronics. Over the past two decades, CNT-containing micro-/nanoelectronics have been used in optical biomedical sensors,[38] thin-film transistors (TFTs),[39,40] sensors,[41] battery electrodes,[42,43] and supercapacitors.[44–46]

Non-conductive metal oxide nanotubes are easily fabricated into low-*k* thin films. Single-walled aluminosilicate nanotubes (AlSiNTs) have a wide bandgap, theoretically exceeding 7.9 eV[47,48] and high intrinsic mechanical strength.[32–35] Fig. 1 presents a cryo-TEM image and the structure of AlSiNTs, which form a material known as synthetic imogolite. The self-assembly mechanism,[49–53] surface properties,[54–56] surface

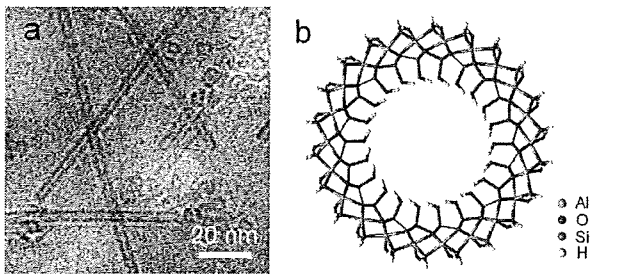

Fig. 1 (a) Cryo-TEM image and (b) illustration of the cross-sectional structure of AlSiNT.

[a]*Department of Chemical Engineering, National Taiwan University, No. 1, Sec. 4, Roosevelt Road, Taipei 10617, Taiwan. E-mail: dunyen@ntu.edu.tw*
[b]*Graduate Institute of Photonics and Optoelectronics, National Taiwan University, No. 1, Sec. 4, Roosevelt Road, Taipei 10617, Taiwan. E-mail: iccheng@ntu.edu.tw*

† Electronic supplementary information (ESI) available: Experimental details, characterization, FTIR, nitrogen physisorption isotherms, and other X-ray scattering results. See DOI: 10.1039/c6nr06106k

Published on 30 September 2016. Downloaded by National Chiao Tung University on 27/10/2016 02:04:51.

charges,[57–60] surface functionalization,[61–64] and applicability[65–68] of these structures have attracted considerable attention over the past five years. Most of the existing AlSiNT-containing thin films are fabricated using poly(vinyl alcohol) (PVA) as the matrix material. PVA makes up approximately 40 wt%[63,64,67,68] of the resulting material, which means that the overall mechanical properties of the thin films are dominated by PVA. PVA has a low Young's modulus (below 1 GPa) when formed into a thin film. Producing low-*k* AlSiNT films with high mechanical strength would require that the thin film be composed predominantly of AlSiNTs. Unfortunately, pure AlSiNT thin films are extremely difficult to produce, due to the poor processability of AlSiNTs.

This paper presents a novel solution process for the fabrication of low-*k* thin films, in which the AlSiNTs make up more than 90 wt% of the resulting material; *i.e.*, the PVA is used primarily as a stabilizer. As such, the dielectric and mechanical properties of the resulting thin films are dominated by the characteristics of the AlSiNTs. Under complete dehydration, the *k* value of the AlSiNT thin films was below 1.5 at a current frequency alternating between 10 and 100 kHz. We conducted controlled rehydration experiments to investigate the degree to which hydration influences the dielectric properties of AlSiNT thin films. Scanning electron microscopy, energy dispersive X-ray spectroscopy, FT-IR spectroscopy, and grazing-incidence X-ray scattering were used to characterize the structure of these films. Nanoindentation was used to characterize the mechanical properties of AlSiNT thin films. We also obtained the refractive index of the AlSiNT thin films in a range of frequencies.

The substrate and solution-cast AlSiNT thin films were imaged using a digital camera, optical microscope (OM), and scanning electron microscope (SEM) (Fig. 2). Fig. 2a presents a photograph of the AlSiNT thin film, which was spin cast from the AlSiNT aqueous solution in the absence of poly(vinyl alcohol) (PVA). The image illustrates the high degree of non-uniformity in the morphology of the thin film (the middle column in Fig. 2a). In contrast, the samples fabricated using 10 wt% of PVA presented a surface morphology of high uniformity. The homogeneity of the cast thin films was further evaluated using top-view OM and SEM images (Fig. 2b and c). The AlSiNT thin film derived from the solution without PVA was unevenly distributed, whereas that derived from the cast solution with PVA was highly uniform. This implies that PVA plays a key role in spin casting, acting as a stabilizer or homogenizer capable of preventing the local aggregation of AlSiNTs during film casting. Severe aggregation is very likely to result in thin films with poor morphological characteristics. The pH of the cast solution went from 6.72 to 5.80. According the previous studies,[58–60] the electrophoretic mobility of the AlSiNTs in the suspension would increase in the presence of PVA. This implied that the cast solution was stabilized by PVA. The cross-sectional SEM image in Fig. 2d presents a homogeneous thin film derived from the AlSiNT solution with PVA on the chromium-coated glass. The thickness of the film is approximately 200 nm. Elemental mapping derived from

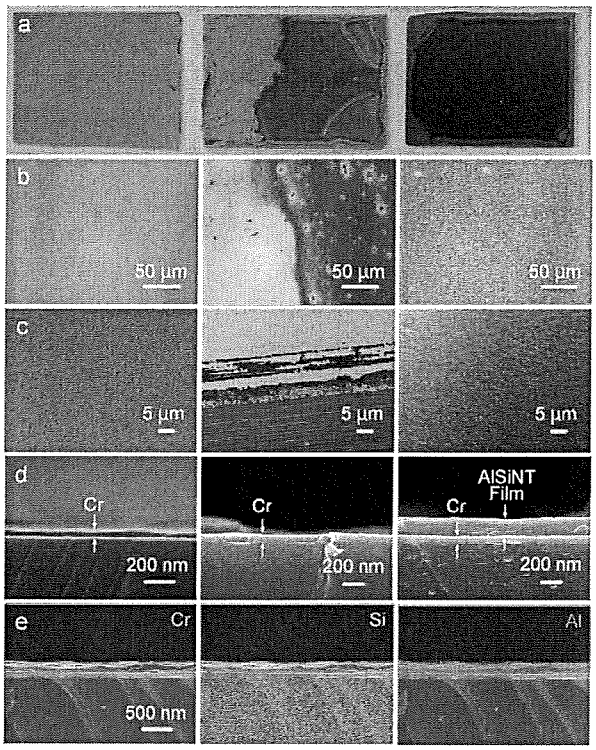

Fig. 2 (a) Photographs, (b) OM images, (c) top-view SEM images and (d) side-view SEM images of the Cr-coated glass substrate (left) of the AlSiNT film spin cast from a solution without PVA (middle) and the AlSiNT film spin cast from a solution with PVA (right). (e) EDS elemental mapping of AlSiNT film spin cast from solution with PVA.

energy dispersive spectroscopy (EDS) was performed for chromium, silicon, and aluminum to confirm that the 200 nm thin film cast from the PVA–AlSiNT solution indeed consisted of AlSiNTs (Fig. 2e). The thin film prepared from the solution with PVA–AlSiNT revealed strong Si and Al signals, which implies the presence of AlSiNTs. The cast aqueous solution comprises AlSiNTs and PVA at a mass ratio of 9 to 1; *i.e.*, the thin film is composed almost entirely of AlSiNTs. In previous studies,[67,68] AlSiNT thin films were produced using a polymer as the matrix (continuous) phase and AlSiNTs as the disperse phase. Polymeric materials are commonly used as the continuous phase in thin films due to the fact that polymers tend to be far easier to process than are AlSiNTs.[67,68] Processing pure AlSiNTs into a uniform thin film can be exceedingly difficult. This is the first report of thin films composed almost entirely of AlSiNTs. The FT-IR spectra of the AlSiNT thin film, PVA in powder form, and the as-synthesized AlSiNTs in powder form are summarized in the ESI, Fig. S1.† The FT-IR spectrum of the AlSiNT thin film revealed the characteristic peaks of PVA and AlSiNTs, further confirming the existence of AlSiNTs in the thin film. The decrease in the absorbance of the OH stretching of the AlSiNT films might be attributed to the formation of hydrogen bonds between the PVA and the external surface of AlSiNTs. Two extended fabrication conditions of

 This journal is © The Royal Society of Chemistry 2016

Published on 30 September 2016. Downloaded by National Chiao Tung University on 27/10/2016 02:04:51.

AlSiNT films were examined: one with poly(ethylene imine) (PEI) as the stabilizer and Cr-coated glass as the substrate, and the other with PVA as the stabilizer and Si wafer as the substrate (ESI, Fig. S2†). Only the latter condition yielded good-quality AlSiNT films, suggesting the critical role of PVA in the thin film fabrication. It is worth mentioning that the dimensions (length and diameter) of AlSiNTs may also affect the thin film fabrication. The control of the dimensions of AlSiNTs has been reported previously.[49,53,69]

Grazing-incidence wide-angle X-ray scattering (GIWAXS) was used to investigate the structure, dispersion, and orientation distribution of AlSiNTs in the thin film prepared from the PVA–AlSiNT solution (Fig. 3). Fig. 3a illustrates the experimental setup using GIWAXS and Fig. 3b presents the 2D GIWAXS patterns. Two pronounced scattering peaks appeared at q_z = 0.33 and 0.65 Å^{-1}. These types of peaks are characteristic and indicative of individually dispersed AlSiNTs.[55,67,68] The GIWAXS pattern with a larger q-range is presented in ESI, Fig. S3.† The absence of diffraction peaks between q_z = 1 and 1.6 Å^{-1} of PVA[68] in the GIWAXS pattern suggests that the PVA formed a dispersed phase in the thin film, and this would be very unlikely to crystallize. A control sample of the AlSiNT film drop cast on a silicon wafer was also subjected to GISAXS analysis (see ESI, Fig. S4†). The film on this sample was much thicker than the spin-cast AlSiNT films discussed in the manuscript. The GISAXS pattern of this control sample is nearly identical to that of the spin-cast sample, suggesting that the X-ray scattering pattern emerges independent of the film thickness. For a more detailed analysis of the AlSiNT dispersion, a 1D scattering pattern was derived from an integration of 2D GIWAXS patterns with respect to χ. In a comparison, the 1D GIWAXS pattern deduced from the experiment was nearly identical to the scattering pattern obtained in simulation based on a model of isolated AlSiNTs (Fig. 3c). This suggests that AlSiNTs in the thin film disperse individually instead of forming small bundles or hexagonal packing. The azimuthal intensity profile of the scattering peak between q = 0.2 and 1 Å^{-1}, also known as the pole figure, was used to analyze the alignment on the nanotubes with respect to the substrate (Fig. 3d). The scattering intensity near χ = 0° represents the horizontal (in-plane) alignment of AlSiNTs, whereas the intensity near χ = 90° represents vertical (out-of-plane) alignment.[68] The highest intensity was found at χ = 0°, suggesting that most of the AlSiNTs are oriented in-plane relative to the surface of the substrate, implying a highly attractive interaction between the external surface of AlSiNTs and the substrate surface.

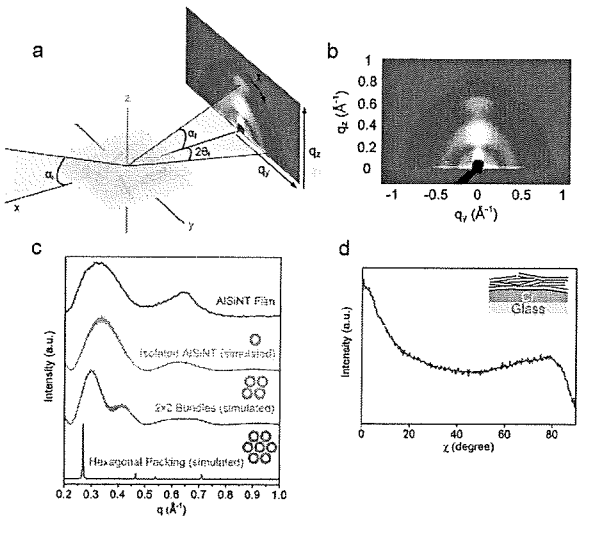

Fig. 3 (a) Illustration showing the configuration of the GIWAXS experiment; (b) 2D GIWAXS pattern of the AlSiNT film spin cast from AlSiNT solution with added PVA; (c) experimentally obtained 1D GIWAXS pattern (top) and simulated WAXS patterns of AlSiNTs with various dispersion characteristics; (d) intensity profiles integrated along the radial direction (0.2 Å^{-1} < q < 1 Å^{-1}) from the raw 2D GIWAXS patterns, as a function of the azimuthal angle (χ).

Fig. 4 presents the relative permittivity (ε_r) of AlSiNT thin films prepared from AlSiNT solution with PVA under various degrees of hydration. The as-cast thin film samples underwent dehydration at 150 °C under vacuum for 12 hours, followed by a rehydration process. Discrete measurements were performed on the as-cast AlSiNT thin film, dehydrated thin film (rehydration time t_h = 0), and rehydrated samples. The dependence of ε_r on t_h was similar at all tested frequencies (Fig. 4a). Specifically, the ε_r of the completely dehydrated sample (t_h = 0) was considerably lower than that of the as-cast sample, and ε_r gradually increased with the rehydration time, t_h. The standard deviations of the ε_r measurements (shown as error bars in Fig. 4a–c) also increased with t_h. The ε_r values at a frequency of 10 kHz were as follows: the as-cast AlSiNT thin film (approximately 13), the completely dehydrated sample (1.05), and the sample rehydrated for 120 min (50). The variation in the ε_r of AlSiNTs as a function of hydration can be explained from three perspectives. First, water has a ε_r value of approximately 80,[70] whereas the ε_r value of typical aluminosilicate materials can be as low as 5.[71] Second, the AlSiNTs are nanoporous aluminosilicate (as indicated by the nitrogen physisorption characterization results in the ESI, Fig. S5†), and higher porosity leads to lower ε_r.[25] Third, the interior surface of AlSiNTs is highly hydrophilic, enabling adsorption of more than 15 wt% of the water.[55] The ε_r of the pure PVA thin film at 100 kHz was measured at 2.26. This is in agreement with the previously reported value.[72] It is worth noting that ε_r = 1.05 in AlSiNT thin films satisfies the criteria for ultra-low-k materials (ε_r < 2.0),[14,17,20] and the value of ε_r is as low as the benchmark ultra-low-k thin film.[8,11,14,23] According to the correlation of the ε_r as a function of the bulk density of zeolites,[73] ε_r of hexagonally packed AlSiNTs at high frequency should be around 1.4. The obtained ε_r of 1.05 might be due to that the AlSiNTs are packed disorderly, as suggested by the GIWAXS characterization. The large surface area of the interstitial spacing due to the disordered packing may also be accessible to the adsorbed water during rehydration. This might result in the remarkable change of ε_r during rehydration. To fabricate AlSiNT thin films whose ε_r is less sensitive to water, the AlSiNTs with a hydrophobic interior surface[64] could be good candidates.

Published on 30 September 2016. Downloaded by National Chiao Tung University on 27/10/2016 02:04:51.

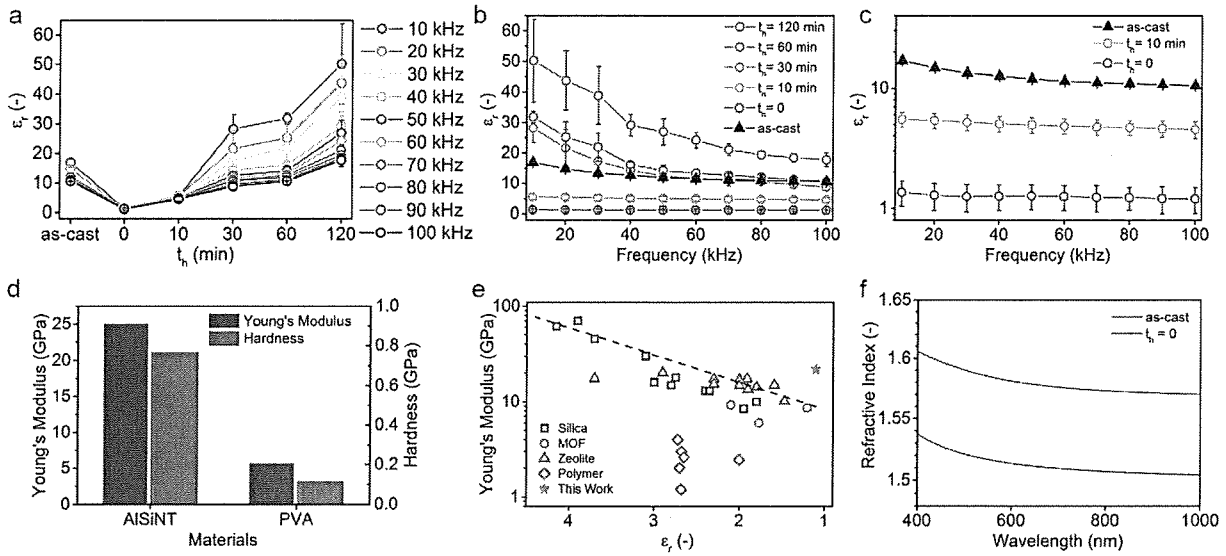

Fig. 4 (a)–(c) Relative permittivity at various t_h values and frequencies; (d) Young's modulus and hardness of the thin film spin cast from AlSiNT solution with added PVA; (e) summary of Young's modulus and relative permittivity of various classes of materials. (f) Refractive index of the as-cast and dehydrated AlSiNT films.

Fig. 4d summarizes the mechanical properties of the AlSiNT thin film, the PVA thin film, and the substrate. The Young's modulus of AlSiNT thin films was 25.1 GPa, which fully satisfies the Young's modulus requirements for the low-k thin film used in electronic devices.[12,13] It is worth noting that the Young's modulus of a single AlSiNT has been computationally predicted to exceed 300 GPa.[33,34] The relatively low Young's modulus of AlSiNT thin films may be because the transverse modulus of nanotubes is usually lower than the longitudinal modulus by one order of magnitude, and the Young's modulus of AlSiNT thin films measured by nanoindentation is likely to be dominated by the transverse modulus of AlSiNTs.[74,75] Fig. 4e summarizes the dielectric and mechanical properties of the AlSiNT thin film and other classes of low-k thin films.[16,18,76,77] Fig. 4e presents the upper-bound of performance for the low-k thin films, indicating a tradeoff between the ε_r and the Young's modulus of common low-k materials. The overall performance of AlSiNT thin films presented in this work transcends the performance upper bound.

Fig. 4f presents the refractive index of the as-cast and dehydrated AlSiNT thin films at various wavelengths. The refractive index of the as-cast AlSiNT thin film was 1.58 at a wavelength of 623 nm, which is very close to the refractive index of 1.52 previously reported for porous aluminosilicate films.[71] The refractive index of the dehydrated AlSiNT film (t_h = 0) was lower than that of the as-cast film. The refractive index of the as-cast as well as dehydrated AlSiNT thin films exhibited normal dispersion characteristics, in that the refractive index decreased with the wavelength. Qualitatively speaking, the refractive index of thin film materials shows a positive correlation with the relative permittivity.[78]

Conclusions

This study developed a solution-based approach to the fabrication of AlSiNT thin films with a uniformly dense layer approximately 200 nm thick on a chromium-coated glass substrate. The grazing-incidence wide-angle X-ray scattering results indicate that most of the AlSiNTs in the film are oriented in the in-plane direction with respect to the substrate. Measurements of the relative permittivity were conducted on the as-cast, dehydrated, and rehydrated AlSiNT films. The dehydrated film presented a relative permittivity of approximately 1.05, which satisfies the criterion for ultra-low-k materials. In contrast, the relative permittivity of the rehydrated AlSiNT thin film exceeded 40, thereby demonstrating the sensitivity of the dielectric properties to the adsorption of water within the AlSiNTs. In addition to the extremely low dielectric constant, these thin films were shown to have mechanical strength far exceeding that of existing low-k materials. Specifically, the Young's modulus of AlSiNT thin films, when measured using a nanoindenter, exceeded 25 GPa. The performance of AlSiNT thin films transcended the trade-off between the relative permittivity and Young's modulus typically found in low-k materials.

Acknowledgements

A.-C. Y., C. H. L., H.-Y. C., and D.-Y. K. acknowledge financial support from the Ministry of Science and Technology (MOST) of Taiwan (MOST 104-2628-E-002-009-MY3 and MOST 105-2923-E-002-002-MY2) and the National Taiwan University (NTU-CDP-105R7814). Y.-S. L. and I.-C. C. acknowledge financial support

 This journal is © The Royal Society of Chemistry 2016

Published on 30 September 2016. Downloaded by National Chiao Tung University on 27/10/2016 02:04:51.

from the Excellent Research Projects of National Taiwan University under Grant NTU-ERP-105R89081. All of the authors acknowledge technical support from beamline 23A in the National Synchrotron Radiation Research Center of Taiwan. Valuable assistance from Hao-Ju Chou and Dr. Cedric Po-Wen Chung in Institute of Chemistry at Academia Sinica in the measurements of nitrogen physisorption is also acknowledged.

Notes and references

1 Y. Chen, G. Zhu, Y. Peng, H. Bi, J. Feng and S. Qiu, *Microporous Mesoporous Mater.*, 2009, **123**, 45–49.
2 E. Kondoh, M. R. Baklanov, H. Bender and K. Maex, *Electrochem. Solid-State Lett.*, 1998, **1**, 224–226.
3 R. D. Miller, *Science*, 1999, **286**, 421–423.
4 K. Maex, M. Baklanov, D. Shamiryan, S. Brongersma and Z. Yanovitskaya, *J. Appl. Phys.*, 2003, **93**, 8793–8841.
5 S. J. Martin, J. P. Godschalx, M. E. Mills, E. O. Shaffer and P. H. Townsend, *Adv. Mater.*, 2000, **12**, 1769–1778.
6 J. Veres, S. D. Ogier, S. W. Leeming, D. C. Cupertino and S. M. Khaffaf, *Adv. Funct. Mater.*, 2003, **13**, 199–204.
7 G. Maier, *Prog. Polym. Sci.*, 2001, **26**, 3–65.
8 C. M. Jin, J. D. Luttmer, D. M. Smith and T. A. Ramos, *MRS Bull.*, 1997, **22**, 39–42.
9 W. L. Wu, W. E. Wallace, E. K. Lin, G. W. Lynn, C. J. Glinka, E. T. Ryan and H. M. Ho, *J. Appl. Phys.*, 2000, **87**, 1193–1200.
10 C. V. Nguyen, K. R. Carter, C. J. Hawker, J. L. Hedrick, R. L. Jaffe, R. D. Miller, J. F. Remenar, H. W. Rhee, P. M. Rice, M. F. Toney, M. Trollsas and D. Y. Yoon, *Chem. Mater.*, 1999, **11**, 3080–3085.
11 S. Yang, P. A. Mirau, C. S. Pai, O. Nalamasu, E. Reichmanis, J. C. Pai, Y. S. Obeng, J. Seputro, E. K. Lin, H. J. Lee, J. N. Sun and D. W. Gidley, *Chem. Mater.*, 2002, **14**, 369–374.
12 H. W. Ro, R. L. Jones, H. Peng, D. R. Hines, H. J. Lee, E. K. Lin, A. Karim, D. Y. Yoon, D. W. Gidley and C. L. Soles, *Adv. Mater.*, 2007, **19**, 2919–2924.
13 K. Zagorodniy, D. Chumakov, C. Taschner, A. Lukowiak, H. Stegmann, D. Schmeier, H. Geisler, H. J. Engelmann, H. Hermann and E. Zschech, *IEEE Trans. Semiconduct. Manufact.*, 2008, **21**, 646–660.
14 S. Eslava, J. W. Seo, C. E. A. Kirschhock, M. R. Baklanov, K. Maex and J. A. Martens, *Adv. Funct. Mater.*, 2010, **20**, 2377–2379.
15 S. Eslava, J. Urrutia, A. N. Busawon, M. R. Baklanov, F. Iacopi, S. Aldea, K. Maex, J. A. Martens and C. E. A. Kirschhock, *J. Am. Chem. Soc.*, 2008, **130**, 17528–17536.
16 Y. Zhu, T. E. Müller and J. A. Lercher, *Adv. Funct. Mater.*, 2008, **18**, 3427–3433.
17 Y. Liu, M. Sun, C. M. Lew, J. Wang and Y. Yan, *Adv. Funct. Mater.*, 2008, **18**, 1732–1738.
18 H. Guo, M. Wang, J. Liu, S. Zhu and C. Liu, *Microporous Mesoporous Mater.*, 2016, **221**, 40–47.
19 S. Eslava, L. Zhang, S. Esconjauregui, J. Yang, K. Vanstreels, M. R. Baklanov and E. Saiz, *Chem. Mater.*, 2013, **25**, 27–33.
20 K. Zagorodniy, G. Seifert and H. Hermann, *Appl. Phys. Lett.*, 2010, **97**, 251905.
21 E. Redel, Z. Wang, S. Walheim, J. Liu, H. Gliemann and C. Wöll, *Appl. Phys. Lett.*, 2013, **103**, 091903.
22 Y. P. Bernal, R. L. Juárez, E. A. D. Vasconcelos, J. E. F. da Silva and W. M. D. Azevedo, *Semicond. Sci. Technol.*, 2015, **30**, 045003.
23 A. T. Cho, F. M. Pan, K. J. Chao, P. H. Liu and J. Y. Chen, *Thin Solid Films*, 2005, **483**, 283–286.
24 T. Jiang, B. Zhu, S.-J. Ding, Z. Fan and D. W. Zhang, *J. Mater. Chem. C*, 2014, **2**, 6502–6510.
25 P. Prabunathan, K. Sethuraman and M. Alagar, *High Perform. Polym.*, 2014, **26**, 283–289.
26 K. Maex, M. R. Baklanov, D. Shamiryan, F. Iacopi, S. H. Brongersma and Z. S. Yanovitskaya, *J. Appl. Phys.*, 2003, **93**, 8793–8841.
27 M. Morgen, E. T. Ryan, J. H. Zhao, C. Hu, T. Cho and P. S. Ho, *Annu. Rev. Mater. Sci.*, 2000, **30**, 645–680.
28 C. W. S. To, *Finite Elem. Anal. Des.*, 2006, **42**, 404–413.
29 Y. Wu, M. Huang, F. Wang, X. M. H. Huang, S. Rosenblatt, L. Huang, H. Yan, S. P. O'Brien, J. Hone and T. F. Heinz, *Nano Lett.*, 2008, **8**, 4158–4161.
30 T. W. Tombler, C. Zhou, L. Alexseyev, J. Kong, H. Dai, L. Liu, C. S. Jayanthi, M. Tang and S.-Y. Wu, *Nature*, 2000, **405**, 769–772.
31 A. Krishnan, E. Dujardin, T. W. Ebbesen, P. N. Yianilos and M. M. J. Treacy, *Phys. Rev. B: Condens. Matter*, 1998, **58**, 14013–14019.
32 T. Gilberto, S. B. Nikolaos, J. F. Andrew, Z. Francesco and A. H. Werner, *J. Phys.: Condens. Matter*, 2009, **21**, 195301.
33 K.-H. Liou and D.-Y. Kang, *ChemNanoMat*, 2016, **2**, 189–195.
34 K.-H. Liou, N.-T. Tsou and D.-Y. Kang, *Nanoscale*, 2015, **7**, 16222–16229.
35 K. J. D. MacKenzie and M. J. Bolton, *J. Mater. Sci.*, 2009, **44**, 2851–2857.
36 S. Iijima, *Nature*, 1991, **354**, 56–58.
37 J. Chen, M. A. Hamon, H. Hu, Y. Chen, A. M. Rao, P. C. Eklund and R. C. Haddon, *Science*, 1998, **282**, 95–98.
38 S. Kruss, A. J. Hilmer, J. Zhang, N. F. Reuel, B. Mu and M. S. Strano, *Adv. Drug Delivery Rev.*, 2013, **65**, 1933–1950.
39 A. Javey, J. Guo, Q. Wang, M. Lundstrom and H. J. Dai, *Nature*, 2003, **424**, 654–657.
40 S. S. Fan, M. G. Chapline, N. R. Franklin, T. W. Tombler, A. M. Cassell and H. J. Dai, *Science*, 1999, **283**, 512–514.
41 J. Kong, N. R. Franklin, C. W. Zhou, M. G. Chapline, S. Peng, K. J. Cho and H. J. Dai, *Science*, 2000, **287**, 622–625.
42 A. S. Arico, P. Bruce, B. Scrosati, J. M. Tarascon and W. Van Schalkwijk, *Nat. Mater.*, 2005, **4**, 366–377.
43 Y. Hou, Y. Cheng, T. Hobson and J. Liu, *Nano Lett.*, 2010, **10**, 2727–2733.
44 A. G. Pandolfo and A. F. Hollenkamp, *J. Power Sources*, 2006, **157**, 11–27.

Published on 30 September 2016. Downloaded by National Chiao Tung University on 27/10/2016 02:04:51.

45 E. Frackowiak and F. Beguin, *Carbon*, 2001, **39**, 937–950.
46 P. Simon and Y. Gogotsi, *Nat. Mater.*, 2008, **7**, 845–854.
47 L. Guimarães, A. N. Enyashin, J. Frenzel, T. Heine, H. A. Duarte and G. Seifert, *ACS Nano*, 2007, **1**, 362–368.
48 M. P. Lourenço, L. Guimarães, M. C. da Silva, C. de Oliveira, T. Heine and H. A. Duarte, *J. Phys. Chem. C*, 2014, **118**, 5945–5953.
49 G. I. Yucelen, D.-Y. Kang, I. Schmidt-Krey, H. W. Beckham and S. Nair, *Chem. Eng. Sci.*, 2013, **90**, 200–212.
50 P. Maillet, C. Levard, O. Spalla, A. Masion, J. Rose and A. Thill, *Phys. Chem. Chem. Phys.*, 2011, **13**, 2682–2689.
51 M. S. Amara, S. Rouzière, E. Paineau, M. Bacia-Verloop, A. Thill and P. Launois, *J. Phys. Chem. C*, 2014, **118**, 9299–9306.
52 A. Thill, P. Maillet, B. Guiose, O. Spalla, L. Belloni, P. Chaurand, M. Auffan, L. Olivi and J. Rose, *J. Am. Chem. Soc.*, 2012, **134**, 3780–3786.
53 G. I. Yucelen, D.-Y. Kang, R. C. Guerrero-Ferreira, E. R. Wright, H. W. Beckham and S. Nair, *Nano Lett.*, 2012, **12**, 827–832.
54 G. I. Yucelen, R. P. Choudhury, J. Leisen, S. Nair and H. W. Beckham, *J. Phys. Chem. C*, 2012, **116**, 17149–17157.
55 D.-Y. Kang, J. Zang, E. R. Wright, A. L. McCanna, C. W. Jones and S. Nair, *ACS Nano*, 2010, **4**, 4897–4907.
56 B. Bonelli, I. Bottero, N. Ballarini, S. Passeri, F. Cavani and E. Garrone, *J. Catal.*, 2009, **264**, 15–30.
57 J. P. Gustafsson, *Clays Clay Miner.*, 2001, **49**, 73–80.
58 C. Castro, N. Arancibia-Miranda, C. Acuña-Rougier, M. Escudey and F. Tasca, *Nanomaterials*, 2016, **6**, 28.
59 N. Arancibia-Miranda, J. Silva-Yumi and M. Escudey, *J. Hazard. Mater.*, 2015, **299**, 675–684.
60 N. Arancibia-Miranda, M. Escudey, M. Molina and M. T. García-González, *J. Non-Cryst. Solids*, 2011, **357**, 1750–1756.
61 C. Zanzottera, M. Armandi, S. Esposito, E. Garrone and B. Bonelli, *J. Phys. Chem. C*, 2012, **116**, 20417–20425.
62 D.-Y. Kang, N. A. Brunelli, G. I. Yucelen, A. Venkatasubramanian, J. Zang, J. Leisen, P. J. Hesketh, C. W. Jones and S. Nair, *Nat. Commun.*, 2014, **5**, 3342.
63 D.-Y. Kang, J. Zang, C. W. Jones and S. Nair, *J. Phys. Chem. C*, 2011, **115**, 7676–7685.
64 I. Bottero, B. Bonelli, S. E. Ashbrook, P. A. Wright, W. Zhou, M. Tagliabue, M. Armandi and E. Garrone, *Phys. Chem. Chem. Phys.*, 2011, **13**, 744–750.
65 E. Paineau, M.-E. M. Krapf, M.-S. Amara, N. V. Matskova, I. Dozov, S. Rouziere, A. Thill, P. Launois and P. Davidson, *Nat. Commun.*, 2016, **7**, 10271.
66 K. Fujikura, H. Maeda, A. Obata, K. Inukai, K. Kato and T. Kasuga, *J. Nanomater.*, 2014, **2014**, 7.
67 D.-Y. Kang, H. M. Tong, J. Zang, R. P. Choudhury, D. S. Sholl, H. W. Beckham, C. W. Jones and S. Nair, *ACS Appl. Mater. Interfaces*, 2012, **4**, 965–976.
68 D.-Y. Kang, M. E. Lydon, G. I. Yucelen, C. W. Jones and S. Nair, *ChemNanoMat*, 2015, **1**, 102–108.
69 S. Konduri, S. Mukherjee and S. Nair, *ACS Nano*, 2007, **1**, 393–402.
70 C. Malmberg and A. Maryott, *J. Res. Natl. Bur. Stand.*, 1956, **56**, 1–8.
71 S. Hietala, D. Smith, V. Hietala and C. Brinker, *J. Mater. Res.*, 1993, **8**, 1122–1127.
72 G. Joshi and S. Pawde, *J. Appl. Polym. Sci.*, 2006, **102**, 1014–1016.
73 R. Poloni and J. Kim, *J. Mater. Chem. C*, 2014, **2**, 2298–2300.
74 S. Yang, S. Yu and M. Cho, *Carbon*, 2013, **55**, 133–143.
75 R. C. Batra and A. Sears, *Modell. Simul. Mater. Sci. Eng.*, 2007, **15**, 835.
76 A. Jain, S. Rogojevic, W. N. Gill, J. L. Plawsky, I. Matthew, M. Tomozawa and E. Simonyi, *J. Appl. Phys.*, 2001, **90**, 5832.
77 M. Johnson, Z. Li, J. Wang and Y. Yan, *Thin Solid Films*, 2007, **515**, 3164–3170.
78 P. Liao, *Theory of Dielectric Optical Waveguides 2e*, Academic Press, 2012.

This journal is © The Royal Society of Chemistry 2016